Particle Accelerators
1978, Vol. 8, pp. 217–224

KLYSTRON INSTABILITY IN THE COAXIAL AUTOACCELERATOR

JOHN G. SIAMBIS and M. FRIEDMAN

Plasma Physics Division, Naval Research Laboratory, Washington, D.C. 20375 USA

(*Received July 7, 1977*)

The klystron instability has been examined for thin solid and thin hollow intense relativistic electron beams inside accelerators composed of cylindrical pipes with periodically spaced accelerating gaps. A stability criterion has been obtained which requires that the gain in velocity modulation from gap to gap be less than one. Application of the stability criteria to preliminary experimental measurements indicates that: (a) if the beam plasma frequency is greater than the fundamental resonant frequency of the coaxial cavities connected to the gaps, and (b) if the ratio of the characteristic impedance of the cavity to the effective local diode impedance of the beam is less than one, then the beam is stable against the klystron instability.

I INTRODUCTION

The stability of electron and ion beams accelerated to high energies by linear accelerators, such as the linear-induction accelerator,[1,2] the traveling-wave accelerator,[3] and the autoaccelerator,[4–10] is a very important design constraint particularly when a high current is desired as well.[2] The instabilities that occur in the beam flow in these accelerating structures have been traditionally divided into two types of interactions:[11] resonant interactions and nonresonant interactions. The resonant interactions,[2] such as the longitudinal bunching mode and the transverse beam breakup mode, have been reexamined in detail in a recent paper by Siambis,[12] with particular emphasis on the slow-wave properties and the spatial harmonics of the accelerating structures. The nonresonant interactions comprise the virtual cathode phenomena and related instabilities,[13] the klystron instability,[14] the resistive wall[15] and inductive wall instabilities.[16]

In this paper we shall examine the klystron instability with particular emphasis on the geometry of the coaxial autoaccelerator at the Naval Research Laboratory.[8] The geometry of the coaxial autoaccelerator in general, Figure 1c, as well as the geometry of the linear-induction accelerator, Figure 1b, resemble the geometry of a multicavity klystron. The multicavity klystron is an amplifier where a signal impressed on the beam as a velocity modulation, at the gap of the first cavity, is amplified many-fold through current bunching and strong coupling to subsequent cavities. In this work stability criteria are derived so that the coaxial autoaccelerator can be designed to operate in a parameter range where the klystron instability is suppressed.

In Section II the analysis of the klystron instability is carried out for the relativistic electron case and for both the high-frequency and low-frequency regimes. In Section III there is discussed a preliminary experiment, in a regime suitable for observing the klystron instability. In Section IV discussion and conclusions are presented.

II ANALYSIS

The geometrical configurations of interest are illustrated in Figures 1b and 1c. The analysis to follow will apply when the gap length, l_g, is much less than the length of the uniform pipe drift region, $l_g \ll l_0 - l_g \approx l_0$. In addition, if the radius of the pipe, r_0, is much less than the length of one cavity section, $r_0 \approx l_g \ll l_0$, then any voltage drop across the gap will be confined axially over an effective distance less than twice the gap length. This has been observed in self-consistent computer simulations of autoacceleration.[17] A strong uniform magnetic field, $B \gtrsim 7$ kG, is assumed in the axial, z, direction. An intense, relativistic electron beam is assumed to flow in the z-direction, with current much less than the critical current[13] I_c. The beam

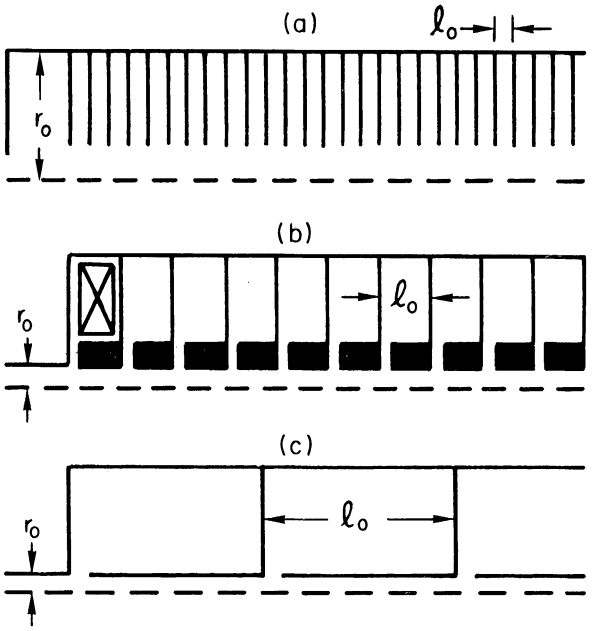

FIGURE 1 Comparative schematic diagrams of linear periodic accelerators; (a) the iris-loaded waveguide; (b) the linear-induction accelerator; (c) the coaxial autoaccelerator.

is either a thin pencil beam on axis, $r_b \ll r_0$, $I \approx 10\ \text{kA} \ll I_c$; or a thin hollow beam near the wall of the drift tube, $\Delta r_b \ll r_b \lesssim r_0$, $I \lesssim 80\ \text{kA} \ll I_c$. The motion of the beam electrons is assumed one-dimensional in the z-direction and the beam is assumed to have no energy transverse to the uniform magnetic field. In proceeding with the analysis we shall assume that the interaction of the electron beam with any sources or sinks across the gap can be considered separately from the free flow of the electron beam in the uniform pipe between any two successive gaps. In addition the quasistatic change in the energy state of the beam at the gap due to autodeceleration or autoacceleration will also be neglected when carrying out the stability analysis.

(a) *First gap interaction*

A voltage of amplitude V_1 and frequency ω is assumed across the first gap. The beam electron is acted by an electric field, E_g, in the z-direction

$$E_g = \left(\frac{V_1}{l_g}\right)\sin \omega t, \qquad -\frac{l_g}{2} < z < \frac{l_g}{2}$$
$$E_g = 0, \qquad |z| > \frac{l_g}{2} \tag{1}$$

Other one-dimensional spatial variations for the electric field at the gap will also be considered after the study of this example. The equation of motion for a beam electron of charge q, velocity u_0, $\beta = u_0/c$, mass γm_0, $\gamma = (1 - \beta^2)^{-1/2}$, is given by

$$\frac{\mathrm{d}(\gamma m_0 u)}{\mathrm{d}t} = qE_g \tag{2}$$

which reduces to

$$\frac{\mathrm{d}u}{\mathrm{d}t} = \frac{qV_1 \sin \omega t}{m_0 \gamma^3 l_g} \tag{3}$$

Integrating in time from t_0, the time the electron enters the gap region, to t_1, the time the electron exits the gap region, we find:

$$u = u_0 + \frac{qV_1}{\omega m_0 \gamma^3 l_g}\left[\cos \omega t_0 - \cos\left(\omega t_0 + \frac{\omega l_g}{u_0}\right)\right]. \tag{4}$$

Next, the origin of time is shifted, $t_0 = t_0 + l_g/2u_0$, to a time origin at the center of the gap, the prime is dropped from the new time variable, and we find:

$$u = u_0 + \delta u = u_0\left[1 + \left(\frac{qV_1}{{u_0}^2 m_0 \gamma^3}\right)M \sin \omega t_0\right]$$
$$M = \frac{\sin(\frac{1}{2}\theta)}{\frac{1}{2}\theta}, \qquad \theta = \frac{\omega l_g}{u_0} \tag{6}$$

which give the velocity modulation of the beam, δu, as a function of the beam parameters, the gap length and the gap voltage and frequency. The quantity M is known as the coupling or modulation coefficient. The effective gap voltage is given by M times V_1. Finite transit time effects of electron motion across the gap are included in M. The assumed rectangular gap field E_g and the resulting coupling coefficient M of Eqs. (1) and (6) constitute a Fourier transform pair which permits finding the coupling coefficient for the general case of gap electric field, by means of its Fourier transform as shown in Ref. 14. The quantity θ is known as the transit angle. Figure 2 shows a plot of M vs θ from Eq. (6), which indicates that in this case the coupling coefficient has an effective bandwidth of $\Omega \approx \pi u_0/l_g$. The fundamental resonant frequency, ω_0, of the coaxial cavity, therefore, must satisfy the condition, $\omega_0 < \Omega$. This condition is easily satisfied for parameters of interest for the coaxial autoaccelerator.[8] High-frequency noise, $\omega > \Omega$, reduces substantially in coupling in and out of the cavity.

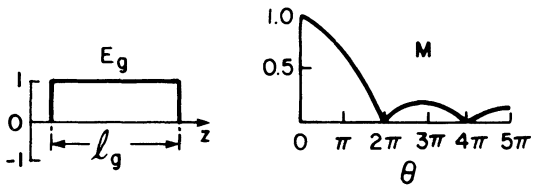

FIGURE 2 The gap electric field E_g and modulation coefficient M.

(b) *Uniform pipe drift region*

The velocity modulation impressed on the beam at the first gap, $(z = 0, t)$, then travels in a long uniform drift section, $(0 < z < l_0)$, before it reaches the next gap, $(z = l_0)$. As a result of the velocity modulation certain groups of particles travel faster than the dc velocity of the beam and other groups of particles travel slower than the dc velocity, u_0. This leads to bunch formation in the drift region. In order to follow this motion and bunch formation, the modulation at the first gap is decomposed into wave excitations on the beam. The propagation of these wave excitations is then followed along the drift region to the second gap. The wave excitations on the beam are constrained to the fast and slow electrostatic plasma waves of the beam.

The dispersion relation for the plasma waves on the beam is given by the following expressions[12,18] for the respective regions of frequency and wave number:

$$1 - \frac{(k^2c^2 - \omega^2)\alpha}{(\omega - ku_0)^2} = 0 \tag{7}$$

for $\omega < \omega_{pr}$, $k \ll k_m = 2\pi/r_0$ and

$$(\omega - u_0 k)^2 = \omega_{pr}^2 \tag{8}$$

for $\omega \gg \omega_{pr}$, $k \gg k_m$, where

$$\omega_{pr}^2 = \frac{\omega_p^2}{\gamma^3} = \frac{q^2 n_e/m_0\varepsilon_0}{\gamma^3} \tag{9}$$

$$\alpha = \frac{I_0}{\beta\gamma^3 I_s} \tag{10}$$

$$I_s = \frac{2\pi\varepsilon_0 m_0 c^2}{q \ln(r_0/r_b)} = \frac{8.5}{\ln(r_0/r_b)}, \quad \text{in kA,} \tag{11}$$

where ω_p is the beam plasma frequency, I_0 is the beam current, and ε_0 the vacuum permitivity.

The high-frequency regime, for the nonrelativistic case, has been extensively explored in connection with the study and design of two-cavity and multicavity klystrons. The relativistic case is derived as follows. The velocity modulation, in the drift region $0 < z < l_0$, is given by

$$\delta u(z, t) = A_f \exp[j(\omega t - k_f z)] + A_s \exp[j(\omega t - k_s z)], \tag{12}$$

where A_f and A_s are constants and are equal to the amplitude of the fast and slow waves respectively. These two constants are set equal, $A_f = A_s = A$. This implies that the current modulation in the first gap is set equal to zero. This is a good assumption, because no bunching occurs within the first gap. The wave numbers k_f and k_s are given by

$$\begin{aligned} k_f &= \frac{\omega}{u_0} - \frac{\omega_{pr}}{u_0} \\ k_s &= \frac{\omega}{u_0} + \frac{\omega_{pr}}{u_0}. \end{aligned} \tag{13}$$

Substitution of Eq. (13) into Eq. (12) yields

$$\delta u(z, t) = 2A \cos\left(\frac{\omega_{pr} z}{u_0}\right) \exp\left[j\left(\omega t - \frac{\omega z}{u_0}\right)\right]. \tag{14}$$

Application of the boundary condition at $z = 0$, gives

$$\delta u(z, t) = -ju_0\left(\frac{qV_1}{u_0^2 m_0 \gamma^3}\right) \times M \cos\left(\frac{\omega_{pr} z}{u_0}\right) \exp\left[j\left(\omega t - \frac{\omega z}{u_0}\right)\right]. \tag{15}$$

The modulation in the beam current δI, is obtained as follows. From the steps leading to the derivation of the dispersion relation we have that

$$\delta I(z, t) = \sum_i \frac{\lambda_0 \omega}{\omega - k_i u_0} \delta u(\omega, k_i, z, t), \tag{16}$$

where λ_0 is the charge per unit length of the unperturbed beam. Next, we find

$$\delta I(z, t) = I_0\left(\frac{\omega}{\omega_{pr}}\right)\left(\frac{qV_1}{u_0^2 m_0 \gamma^3}\right) \times M \sin\left(\frac{\omega_{pr} z}{u_0}\right) \exp\left[j\left(\omega t - \frac{\omega z}{u_0}\right)\right]. \tag{17}$$

Before discussing Eqs. (15) and (17), another quantity, the beam kinetic voltage, $\delta V(z, t)$, which

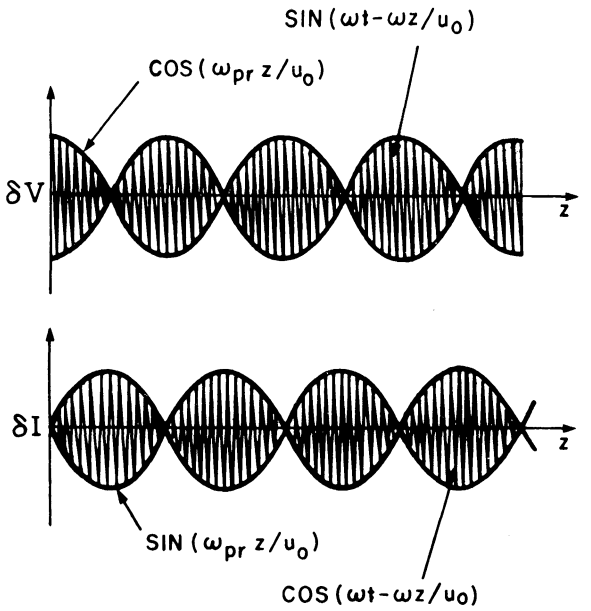

FIGURE 3 Standing wave pattern of (a) kinetic voltage δV and (b) current bunching δI in the drift region.

is simply related to the velocity modulation, is introduced.

$$\delta V(z, t) \equiv \left(\frac{u_0 m_0 \gamma^3}{q}\right)\delta u(z, t)$$
$$= -jV_1 M \cos\left(\frac{\omega_{pr} z}{u_0}\right)\exp\left[j\left(\omega t - \frac{\omega z}{u_0}\right)\right]. \tag{18}$$

Figure 3 shows the amplitude variation of $\delta V(z, t)$ and $\delta I(z, t)$ along the drift region. It is seen that the bunching in velocity or kinetic voltage is spatially 90 degrees out of phase with the bunching in the beam current. For klystron operation it is required that the second gap be placed at a current bunching location, i.e.,

$$\frac{\omega_{pr} l_0}{u_0} = \frac{n\pi}{2}; \qquad n = 1, 3, \ldots. \tag{19}$$

For the low-frequency regime, $\omega < \omega_{pr}$, we proceed as follows. From the dispersion relation of Eq. (7), we obtain the fast- and slow-wave wavenumbers,

$$k_f = \frac{\omega}{u_0}\frac{1 + \alpha}{1 + \alpha\mu}$$
$$k_s = \frac{\omega}{u_0}\frac{1 + \alpha}{1 - \alpha\mu}, \tag{20}$$

where

$$\mu = \frac{[1 + (1 - \beta)/\alpha]^{1/2}}{\beta} \tag{21}$$

and

$$\alpha \ll 1.$$

If we follow the procedure of Eqs. (12), (14)–(18), and assume that $A_f = A_s$, then the resulting equation of $\delta I(z, t)$ will have a nonzero component at the first gap, which is in phase, spatially and temporally with the velocity modulation. This is due to the fact that the low-frequency fast and slow wave branches are asymmetric around the beam line, $\omega = ku_0$. This asymmetry comes from the factor, $1 + \alpha$, in the right-hand side of Eq. (20). In order to keep the current modulation equal to zero in the first gap, because it takes time for the velocity modulation to result in bunching and current modulation, the level of excitation of the fast wave A_f, and the slow wave A_s will now be assumed different, $A_f \neq A_s$, for the low-frequency regime. Repeating the procedure we find

$$\delta V(z, t) = -jV_1 M\left[\cos\left(\frac{\omega\xi z}{u_0}\right) - j\zeta \sin\left(\frac{\omega\xi z}{u_0}\right)\right]\exp\left[j\left(\omega t - \frac{\omega\xi z}{u_0}\right)\right]. \tag{22}$$

$$\delta I(z, t) = I_0\left[\frac{1 - \alpha^2\mu^2}{\alpha\mu(1 + \alpha)}\right]\left(\frac{qV_1}{u_0^2 m_0 \gamma^3}\right) \times M \sin\left(\frac{\omega\xi z}{u_0}\right)\exp\left[j\left(\omega t - \frac{\omega\xi z}{u_0}\right)\right], \tag{23}$$

where

$$\xi = \frac{1 + \alpha}{1 - \alpha^2\mu^2} \approx 1 \tag{24}$$

and

$$\zeta = \frac{1 + \alpha\mu^2}{\mu(1 + \alpha)} < 1. \tag{25}$$

Equation (22) shows that now the velocity or voltage modulation has a new component 90 degrees out of phase in space and time from the standard term. The presence of this term is due to the asymmetry of the fast and slow wave branches around the beam line for the low-frequency regime. If the two branches of the low-frequency dispersion relation are symmetrized, by fiat, around

the beam line, by dropping the α, $\alpha \ll 1$, in the $1 + \alpha$ term in Eq. (20), then the new term in the kinetic voltage modulation is zero and the standard terms have nearly the same amplitude as given in Eqs. (22) and (23).

(c) *Second gap interaction, high frequency.*

For proper klystron operation, that is maximum amplification at the second gap of the input signal V_1 from the first gap, the length l_0 between gaps is chosen according to Eq. (19). For stable accelerator operation on the other hand, the distance l_0 must be such that

$$\frac{\omega_{pr} l_0}{u_0} = \frac{n\pi}{2}, \qquad n = 2, 4, \ldots \tag{26}$$

so that there is no current bunching at the second and subsequent gaps. The length, l_0, however is not a free parameter. Also the relativistic beam-plasma frequency varies both with beam current and the γ of the beam. It is therefore necessary to assume that some beam-current bunching occurs at the second gap. Next we rewrite δI and δV at the input of the second gap, l_{0-}, leaving out the fast phase variation, $-j \exp[j(\omega t - \omega l_0/u_0)]$

$$\delta I(l_{0-}) = j\left(\frac{V_1}{Z_0}\right)\sin k_p l_0 \tag{27}$$

$$\delta V(l_{0-}) = V_1 \cos k_p l_0 \tag{28}$$

$$Z_0 = \left(\frac{\omega_{pr}}{\omega}\right)\left[\frac{(u_0^2 m_0 \gamma^3/q)}{I_0}\right] \tag{29}$$

$$k_p = \frac{\omega_{pr}}{u_0}, \tag{30}$$

where Z_0 is the characteristic impedance of the beam perturbations in the drift tube. The gap and its cavity will appear to the bunched beam current as a shunt resistance, R_{sh}, as shown in Figure 4.

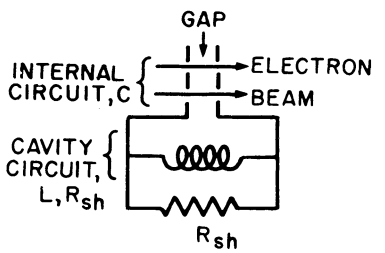

FIGURE 4 Equivalent circuit for the gap and the cavity. C is the capacitive coupling across the gap in the drift tube. L and R_{sh} are the inductance and shunt resistance or characteristic impedance of the cavity.

The bunched beam current in going through the gap will suffer a phase shift θ, as well as induce a voltage on the gap equal to $V_2 = MR_{sh}\delta I(l_0)$, which in turn will produce a kinetic voltage modulation on the beam, $\delta V(l_{0+})$, given by

$$\delta I(l_{0+}) = \delta I(l_{0-})e^{-j\theta} \tag{31}$$

$$V_2 = MR_{sh}\delta I(l_{0-})e^{-j\theta/2} \tag{32}$$

$$\delta V(l_{0+})|_{new} = -M^2 R_{sh}\delta I(l_{0-})e^{-j\theta} \tag{33}$$

$$\delta V(l_{0+})|_{old} = \delta V(l_{0-})e^{-j\theta} \tag{34}$$

At the output of the second gap, leaving out the phase variation, $\exp(-j\theta)$, we now have

$$\delta V(l_{0+}) = -jGV_1 \sin k_p l_0 + V_1 \cos k_p l_0 \tag{35}$$

$$\delta I(l_{0+}) = j\left(\frac{V_1}{Z_0}\right)\sin k_p l_0 \tag{36}$$

$$G = \frac{M^2 R_{sh}}{Z_0} = \left(\frac{\omega}{\omega_{pr}}\right)\frac{M^2 R_{sh} I_0}{(u_0^2 m_0 \gamma^3/q)}. \tag{37}$$

The quantity G, is the well known gain in velocity modulation from klystron theory. The first term in δV is the cascade term, the second term is the feedthrough term. The effective gain is defined by

$$G_{eff} = \left|\frac{\delta V(l_{0+})}{V_1}\right| = [1 + (G^2 - 1)\sin^2 k_p l_0]^{1/2}. \tag{38}$$

If $G > 1$, then the kinetic voltage has increased and a klystron amplifier type of operation is obtained leading to instability for the case of accelerator operation. If $G < 1$, then we obtain a stable accelerator regime. A sufficient, therefore, condition for stability is

$$G < 1. \tag{39}$$

(d) *Second gap interaction, low frequency*

For the low-frequency regime the relevant quantities at the output of the second gap are given by

$$\delta V(l_{0+}) = -jG'V_1 \sin k'_p l_0 + V_1 \cos k'_p l_0 - jV_1\zeta \sin k'_p l_0 \tag{40}$$

$$\delta I(l_{0+}) = j\frac{V_1}{Z'_0}\sin k'_p l_0 \tag{41}$$

$$Z'_0 = \left[\frac{\alpha\mu(1+\alpha)}{(1-\alpha^2\mu^2)}\right]\left[\frac{u_0^2 m_0 \gamma^3/q}{I_0}\right] \tag{42}$$

$$k'_p = \left(\frac{\omega}{u_0}\right)\left[\frac{\alpha\mu}{(1-\alpha^2\mu^2)}\right] \tag{43}$$

$$G' = \frac{M^2 R_{sh}}{Z'_0} = \left[\frac{(1-\alpha^2\mu^2)}{\alpha\mu(1+\alpha)}\right]\left[\frac{M^2 R_{sh}/I_0}{(u_0^2 m_0 \gamma^3/q)}\right]. \tag{44}$$

The effective kinetic voltage gain is then given by

$$G'_{eff} = \{1 + [(G' + \zeta)^2 - 1]\sin^2 k'_p l_0\}^{1/2}. \tag{45}$$

The condition for stability is

$$G' + \zeta < 1. \tag{46}$$

The presence of the feedthrough term, $\zeta < 1$, now renders the stability condition a more difficult one to satisfy, despite the fact that $G' < G$ (minimum), because $Z'_0 > Z_0$ (maximum). But even in cases when the stability condition of Eq. (46) is not satisfied the resulting effective gain, G'_{eff}, can be very small because of the sine squared term in Eq. (45). The argument of this term is written in terms of $k'_p = 2\pi/l'_p$,

$$l'_p = \left(\frac{c}{f_0}\right)\frac{(1-\alpha^2\mu^2)}{\alpha\mu} \gg l_0, \tag{47}$$

where the fundamental resonant frequency of the cavity is given in terms of the transit time τ_0 of the cavity by

$$f_0 = \frac{1}{4\tau_0} = \frac{c}{4l_0} \tag{48}$$

so that

$$\sin^2 k'_p l_0 = \sin^2\left[\frac{\pi}{2}\frac{\alpha\mu}{(1-\alpha^2\mu^2)}\right] \approx \left[\frac{\pi}{2}\frac{\alpha\mu}{(1-\alpha^2\mu^2)}\right]^2 \ll 1. \tag{49}$$

The above relation places an upper limit on the length, l_s, of one section of the autoaccelerator, when $G'_{eff} > 1$,

$$\frac{l_s}{l_0} < \frac{(1-\alpha^2\mu^2)}{\alpha\mu}. \tag{50}$$

(e) *Discussion of gain*

We have seen so far what happens at the output of the second gap. This procedure must be repeated for all subsequent gaps. In doing so the analysis quickly gets out of hand. Instead we focus attention on the expressions for the gain, given by Eqs. (37) and (44), and will investigate the conditions which make the gain less than one. These two expressions have a common factor, namely,

$$\frac{M^2 R_{sh} I_0}{(u_0^2 m_0 \gamma^3/q)}.$$

The value of M is always less than one, see Figure 2. The value of the shunt resistance R_{sh} is equal to the characteristic impedance per unit length of the coaxial cavity

$$R_{sh} = Z_c = cL_c = 60 \ln\left(\frac{r_c}{r_0}\right), \text{ ohms}, \tag{51}$$

where L_c is the inductance per unit length of the coaxial cavity and r_c, r_0 are the outer and inner radii of the coaxial cavity. A typical value for the proposed autoaccelerator and the experiment of Section III is $Z_c \approx 80$ ohms. The remaining quantity

$$\frac{(u_0^2 m_0 \gamma^3/q)}{I_0} = 2Z_D \tag{52}$$

is twice the diode impedance for the nonrelativistic regime, $\gamma \to 1$. For the relativistic case, $\gamma \gg 1$, and also when autodeceleration or autoacceleration takes place in the gap regions as well, then this ratio defines an equivalent local diode impedance, Z_D. In order to keep the gain less than one, in both frequency regimes, the ratio of the cavity characteristic impedance to the beam equivalent local diode impedance must be minimized. The remaining factor in the expression for the high-frequency gain is $\omega/\omega_{pr} = \omega_0/\omega_{pr}$, for $\omega_0 > \omega_{pr}$. Clearly the minimum value of this factor is 1. However this minimum value might not be attainable because the corresponding factor in the expression for the low-frequency gain, $(1-\alpha^2\mu^2)/\alpha\mu(1+\alpha)$, which is independent of frequency, may have a higher value which then automatically becomes the minimum actual value for the high-frequency expression as well. From this discussion it becomes evident that in order to insure stability against the klystron instability the ratio of the cavity characteristic impedance to the equivalent local diode impedance must be minimized and the ratio of the fundamental resonant frequency of the cavity to the beam-plasma frequency must be minimized, so that the product of these two ratios is less than one. Conversely a regime of high gain is obtained when

$$\left(\frac{\omega_0}{\omega_{pr}}\right)\left(\frac{Z_c}{2Z_D}\right)M^2 \gg 1 \tag{53}$$

as in klystron operation.

III EXPERIMENT

A preliminary experiment that illuminates the klystron instability and its relationship to the stability criteria derived here has been performed before the theoretical results were obtained.

The geometrical arrangement of the drift tube and coaxial cavities is identical to that of Refs. 19 and 20. In this experiment the phenomenon of automodulation was demonstrated. The drift tube consisted of a 1.2 meter long, 4.7 cm i.d. stainless-steel tube. Four gaps, feeding four coaxial cavities in sequence, were cut into the drift tube. The length of each cavity was 15 cm and its outer diameter was 18 cm. The fundamental resonant frequency of these cavities was $f_0 = 500$ MHz, which is much higher than the resonant frequency, $f_0 = 75$ MHz, suitable for the autoacceleration interaction of Refs. 6–10. The injected electron beam is a thin, annular beam near the drift tube wall, $r_b \approx 1.9$ cm, $\Delta r_b \approx 0.2$ cm. The electron beam parameters are indicated in Figure 5. Figure 5a shows the time profile of the diode voltage. The voltage rises from 0 to 250 kV in 0.7 μsec. Figure 5b shows the signal picked up by a magnetic probe inside the fourth and last cavity. The average value of the signal is proportional to the beam current at the location of the fourth gap, which is seen to rise from 0 to 5 kA in 0.7 μsec. Figure 5b also shows a large amplitude signal of frequency $f \approx 500$ MHz, equal to the fundamental resonant frequency of the cavities. When the beam current reaches approximately 4 kA, then the beam plasma frequency $f_{pr} \approx f_0 \approx 500$ MHz and the klystron oscillation reduces substantially to low-level noise amplitude and remains for the remainder of the beam pulse, where $f_{pr} > f_0$. The ratio of the characteristic impedance of the cavity, $Z_c \approx 80$ ohms, to the effective local diode impedance, $Z_D \approx 50$ ohms, is

$$\frac{Z_c}{2Z_D} \approx 0.8. \tag{54}$$

The value of the coupling coefficient is $M \approx 1$. Applying these values to Eq. (53) it is concluded that for $f_0 > f_{pr}$, this experiment should show large amplitude klystron oscillations as it does, while for $f_0 \lesssim f_{pr}$, the klystron oscillations should be suppressed as is apparent from Figure 5b.

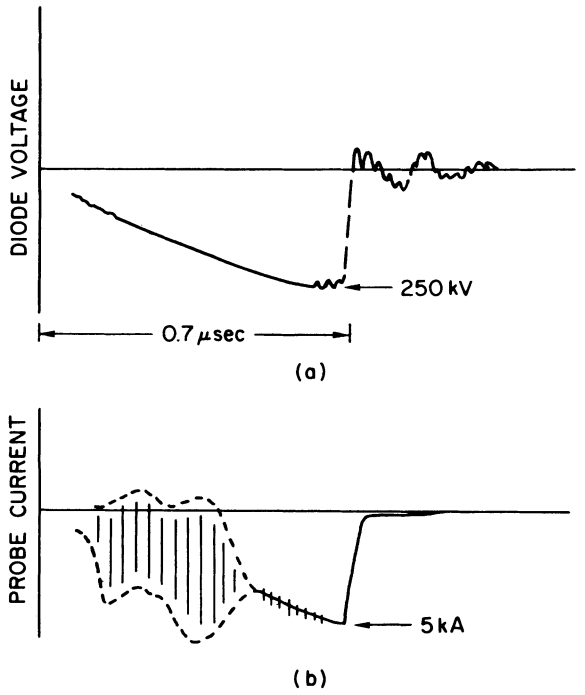

FIGURE 5 (a) Diode voltage versus time and (b) magnetic probe current in the last cavity.

IV CONCLUSIONS

In Section II there have been obtained stability criteria for the klystron instability. For the high-frequency regime, the stability criterion of Eq. (39), is an extension to relativistic energies of the well-known result for amplification in klystron tubes. For the low-frequency regime, the stability criterion of Eq. (44) and adjoining discussion are a new result covering a regime of operation of no interest in klystron tubes, because of the low gain G, due to high beam impedance and because of the difficulty in satisfying the optimum spatial conditions for high effective gain with gap spacing of reasonable length.

In Section III a preliminary experiment has been presented. The stability criteria have been applied to the experimental results and reasonable agreement has been obtained for the onset of suppression of the klystron instability.

In order to suppress the klystron instability attention must be given to the following parameters. The fundamental resonant frequency of the cavity must be less than the beam-plasma frequency. The characteristic cavity impedance must be less than twice the effective local diode impedance. The α-parameter of the beam, Eqs. (10) and

(11), must be as small as possible. This last constraint implies thin hollow beams near the drift-tube wall when very intense currents are needed as is the case with the charging beam for the auto-accelerator. The γ of the charging beam must also be held to as high a value of γ as practical in order to keep α as small as possible. The smallness of the α-parameter also insures a small ratio of beam current to critical current.

ACKNOWLEDGMENTS

The authors acknowledge with pleasure useful discussions with R. Briggs, A. Drobot, T. Godlove, and V. K. Neil. This work was supported by the Office of Naval Research.

REFERENCES

1. J. W. Beal et al., *IEEE Trans. Nucl. Sci.*, **NS-16**, 294 (1969).
2. V. K. Neil and R. K. Cooper, *Particle Accelerators*, **1**, 111 (1970).
3. R. Helm, Proc. 1966 Linear Accelerator Conf., Los Alamos, p. 254.
4. L. Kazanskii et al., *At. Energ.* **30**, 27 (1971).
5. R. J. Briggs et al., Proc. Ninth Intern. Conf. on High Energy Accelerators, p. 278, 1974.
6. M. Friedman, *Phys. Rev. Lett.* **31**, 1107 (1973).
7. J. Siambis, *Phys. Fluids* **19**, 1784 (1976).
8. J. K. Burton et al., *IEEE Trans. Nucl. Sci.*, **NS-24**, 1628 (1977).
9. V. A. Bashmokov et al., *Zh, Tekh. Fiz.* **43**, 1092 (1973) [*Sov. Phys.-Tech. Phys.* **18**, 696 (1973)].
10. I. A. Grishaev et al., *Zh. Tekh. Fiz.* **44**, 1743 (1974) [*Sov. Phys.-Tech. Phys.* **19**, 1087 (1975)].
11. V. K. Neil, private communication.
12. J. G. Siambis, *Particle Accelerators*, **8**, 211 (1978).
13. M. Friedman et al., *Appl. Phys. Lett.* **28**, 308 (1976).
14. C. K. Birdsall and W. B. Bridges, *Electron Dynamics of Diode Regions* (Academic Press, New York, 1966), Chapter 4.
15. V. K. Neil and A. M. Sessler, *Rev. Sci. Instrum.* **36**, 429 (1965) and L. J. Laslett et al, *Rev. Sci. Instrum.* **36**, 436 (1965).
16. V. K. Neil and R. J. Briggs, *Plasma Phys.* **9**, 631 (1967).
17. A. Drobot and J. Siambis, to be published.
18. R. J. Briggs, *Phys. Fluids* **19**, 1257 (1976).
19. M. Friedman, *Phys. Rev. Lett.* **32**, 92 (1974).